JPEDAV (2009) 30:127–135
DOI: 10.1007/s11669-009-9470-9
1547-7037 ©ASM International

Activities in the $FeTiO_3$-$NiTiO_3$ Solid Solution from Alloy-Oxide Equilibria at 1273 K

K.T. Jacob, Shubhra Raj, and S.N.S. Reddy

(Submitted April 4, 2008; in revised form January 12, 2009)

Nine tie-lines between Fe-Ni alloys and $FeTiO_3$-$NiTiO_3$ solid solutions were determined at 1273 K. Samples were equilibrated in evacuated quartz ampoules for periods up to 10 days. Compositions of the alloy and oxide phases at equilibrium were determined by energy-dispersive x-ray spectroscopy. X-ray powder diffraction was used to confirm the results. Attainment of equilibrium was verified by the conventional tie-line rotation technique and by thermodynamic analysis of the results. The tie-lines are skewed toward the $FeTiO_3$ corner. From the tie-line data and activities in the Fe-Ni alloy phase available in the literature, activities of $FeTiO_3$ and $NiTiO_3$ in the ilmenite solid solution were derived using the modified Gibbs-Duhem technique of Jacob and Jeffes [K.T. Jacob and J.H.E. Jeffes, An Improved Method for Calculating Activities from Distribution Equilibria, *High Temp. High Press.*, 1972, 4, p 177-182]. The components of the oxide solid solution exhibit moderate positive deviations from Raoult's law. Within experimental error, excess Gibbs energy of mixing for the $FeTiO_3$-$NiTiO_3$ solid solution at 1273 K is a symmetric function of composition and can be represented as:

$$\Delta G^{E} = 8590\,(\pm 200)\,X_{FeTiO_3}\,X_{NiTiO_3} \quad \text{J/mol}$$

Full spectrum of tie-lines and oxygen potentials for the three-phase equilibrium involving Fe-Ni alloys, $FeTiO_3$-$NiTiO_3$ solid solutions, and TiO_2 at 1273 K were computed using results obtained in this study and data available in the literature.

Keywords ilmenite solid solution, lattice parameters, oxygen potential diagram, phase equilibria, system Fe-Ni-Ti-O, thermodynamic activities

1. Introduction

Thermodynamic data on titanates and their solid solutions are important for understanding metal-support interactions in M/TiO_2 catalysts,[1] stability domains of anodes for photoelectrolysis of water,[2,3] and a new generation of solid-state lubricants.[4] Optimization of the processes for the recovery of metals and alloys from ilmenite minerals also requires thermodynamic input. As part of a larger program of research on ternary oxides and their solid solutions, phase equilibria were explored in part of the Fe-Ni-Ti-O quaternary system at 1273 K. Studies on phase equilibria in the oxide systems MnO-CoO-TiO_2 and MnO-NiO-TiO_2 at 1523 K were reported earlier by Evans and Muan.[5]

K.T. Jacob, and **Shubhra Raj,** Department of Materials Engineering, Indian Institute of Science, Bangalore 560 012, India; **S.N.S. Reddy,** Semiconductor Research and Development Center, IBM Corporation, Hudson Valley Research Park, Hopewell Junction, NY 12533, USA. Contact e-mail: katob@materials.iisc.ernet.in.

2. Experimental Procedure

2.1 Preparation

Fe-Ni alloys were prepared by melting together metals of 99.99% purity in yttria-stabilized zirconia crucibles under ultrahigh purity argon. The argon gas of 99.999% purity was first dried by passing through silica gel, anhydrous $Mg(ClO_4)_2$, and P_2O_5, and then deoxidized by passing through copper wool at 723 K and titanium granules at 1100 K. Alloy powders were prepared from the quenched ingot by filing. Nickel titanate ($NiTiO_3$) was synthesized from NiO and TiO_2 by the solid-state ceramic route. Iron titanate ($FeTiO_3$) was prepared by intimately mixing Fe, Fe_2O_3, and TiO_2 in the appropriate molar ratio and reacting the compacted mixture at 1373 K for 3 days. The pellets were contained in a zirconia crucible, which was sealed inside an evacuated silica quartz ampoule. After the first heat treatment, the pellet was ground, repelletized, and heat treated again under identical conditions for a further period of 3 days. After each heat treatment, a thin layer of the pellet in contact with the zirconia crucible was removed by grinding to minimize contamination. X-ray powder diffraction (XRPD) indicated the formation of single-phase titanates with ilmenite structure (space group $R\bar{3}$). The structure can be visualized as a nearly close-packed hexagonal lattice with cations occupying $^2/_3$ of the octahedral interstices. Solid solutions were prepared in a similar way by heat treating intimate mixtures of nickel and iron titanates at 1473 K.

2.2 Equilibration

Precisely weighed quantities of selected alloy and oxide solid-solution powders were pressed into a pellet and placed in a zirconia crucible. The crucible was put into a quartz tube, which was rinsed three times under vacuum (~1 Pa) with pure argon and then flame sealed under vacuum. Powders of the alloy and oxide solid solution were mixed in approximately equimolar ratio and pelletized at 200 MPa pressure in a steel die. In preliminary experiments, the initial compositions of the two phases were selected such that the mole fraction of $FeTiO_3$ in the oxide solid solution was approximately 30 times higher than the mole fraction of Fe in the alloy because of the relatively higher stability of $FeTiO_3$ compared to $NiTiO_3$. In subsequent experiments, the compositions were chosen using the equilibrium composition ratios established in earlier runs.

2.3 Chemical Analysis

Part of the quenched sample was mounted and polished for energy-dispersive x-ray spectroscopy (EDS) and optical microscopy. Part of the sample was analyzed by XRD. Mixed with powder sample for XRD was elemental silicon, which acted as an internal standard, so that accurate cell dimensions can be obtained by least-squares refinement of lattice spacings. The variation of the lattice parameters of the titanate solid solution with composition is shown in Fig. 1 and 2. Within experimental uncertainty, the lattice parameters vary linearly with composition in conformity with Vegard's approximation. These calibration plots were used to assess the composition of the titanate phase in equilibrated samples. Quantitative analysis of individual phases was done by EDS on a JEOL 7830F Auger Microprobe (JEOL, Japan). A narrow electron beam was focused on either the oxide or alloy phase to minimize the interference from neighboring phases. Pure Fe, Ni, and TiO_2 were used for calibration.

3. Results and Discussion

3.1 Tie Lines

The Fe-Ni alloys coexist with the ilmenite solid-solution $FeTiO_3$-$NiTiO_3$. Experimental tie-line compositions of the alloy and the oxide solid solution at 1273 K are summarized in Table 1 and displayed in Fig. 3. The upper scale allows the alloy composition to be read more accurately. The tie-lines are skewed toward the $FeTiO_3$ corner. Attainment of equilibrium was verified by the conventional tie-line rotation technique as demonstrated in Fig. 4. After a tie-line was experimentally determined, a set of compositions of alloy and ilmenite solid solution on opposite sides of the tie-line were selected and mixed in the required ratio to produce a sample with the same average composition. The selected compositions are joined with a dotted line (a) in Fig. 4. The sample was equilibrated first for 5 days and then for another 5 days. During equilibration the compositions of the two phases were found to move toward the equilibrium

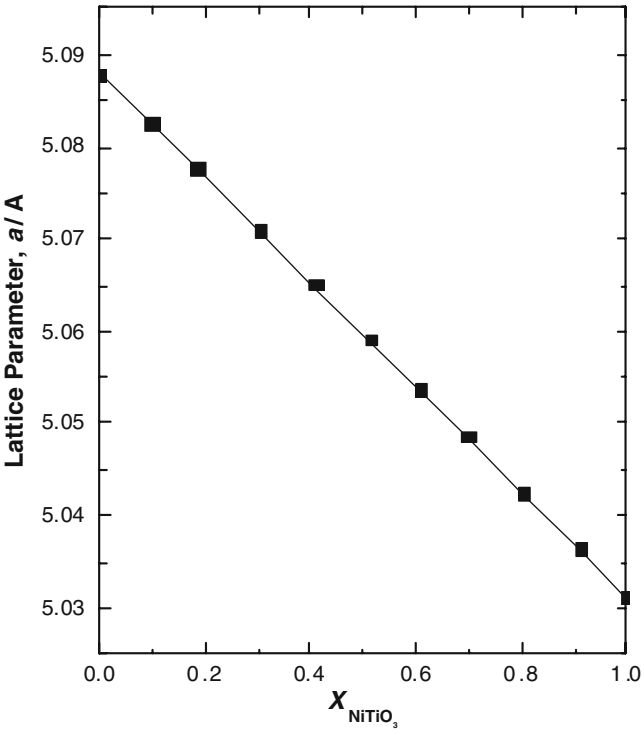

Fig. 1 Variation of the lattice parameter, *a*, with composition of the titanate solid solution

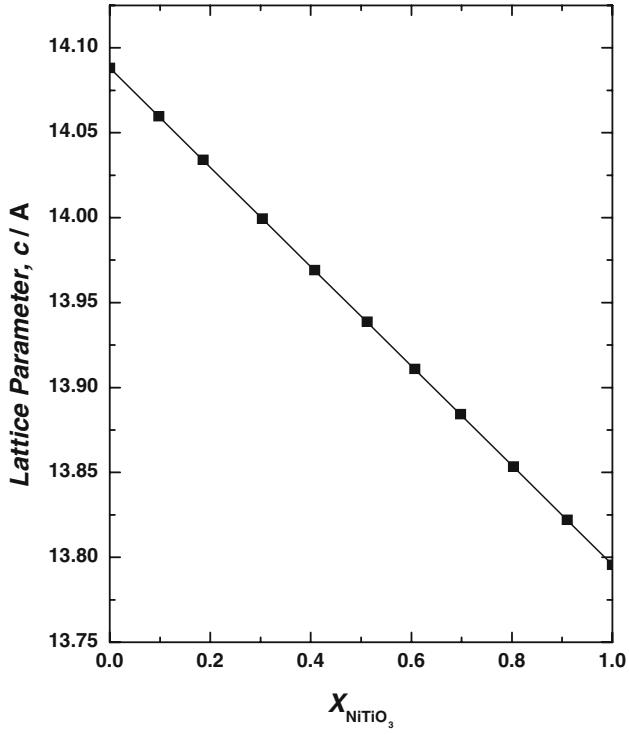

Fig. 2 Variation of the lattice parameter, *c*, with composition of the titanate solid solution

value, and the dotted line connecting the actual compositions of the two phases at any given time was found to rotate toward the equilibrium tie-line. The experiment was repeated starting with a set of compositions corresponding to the dotted line (b) on the opposite side of the equilibrium tie-line as shown in the figure. When compositions from opposite sides converged, attainment of equilibrium was ascertained.

Table 1 Compositions of the $FeTiO_3$-$NiTiO_3$ solid solution in equilibrium with Fe-Ni alloy at 1273 K

Composition of the oxide solid solution, X_{FeTiO_3}	Composition of the alloy phase, X_{Fe}	Ratio of the activity coefficients of the alloy phase (a), γ_{Fe}/γ_{Ni}
0.116	0.00281	0.1862
0.184	0.00405	0.1891
0.286	0.00621	0.1903
0.386	0.00822	0.1928
0.512	0.01149	0.1974
0.676	0.01658	0.2036
0.766	0.02153	0.2110
0.870	0.03241	0.2255
0.944	0.06139	0.2661

(a) From Ref 9

3.2 Thermodynamic Properties of the Oxide Solid Solution

The standard Gibbs energy of formation of $FeTiO_3$ according to the reaction,

$$Fe + {}^1/_2O_2 + TiO_2 \rightarrow FeTiO_3. \quad \text{(Eq 1)}$$

has been accurately measured by Jacob and Kale.[6] For 1184 K < T < 1275 K

$$\Delta G_1^o = -294405 + 47.547T + 3.783T \ln T \quad \text{J/mol} \quad \text{(Eq 2)}$$

For the formation of $NiTiO_3$ according to the reaction,

$$Ni + {}^1/_2O_2 + TiO_2 \rightarrow NiTiO_3 \quad \text{(Eq 3)}$$

the standard Gibbs energy change is given by Jacob et al.[7]

$$\Delta G_3^o = -503468 + 253.283T - 9.796T \ln T \quad \text{J/mol} \quad \text{(Eq 4)}$$

The formation of the solid solution between $FeTiO_3$ and $NiTiO_3$ involves the mixing of one Fe^{2+} and Ni^{2+} on a

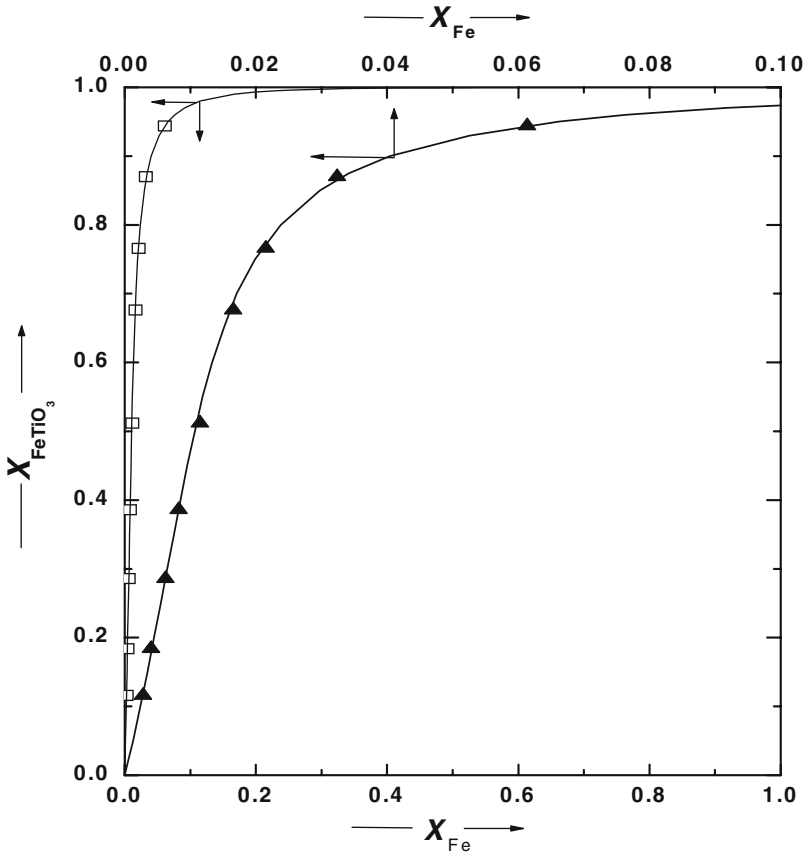

Fig. 3 Relation between compositions of coexisting alloy and ilmenite solid solution phases at 1273 K. The lower curve shows the low concentration data on an expanded scale

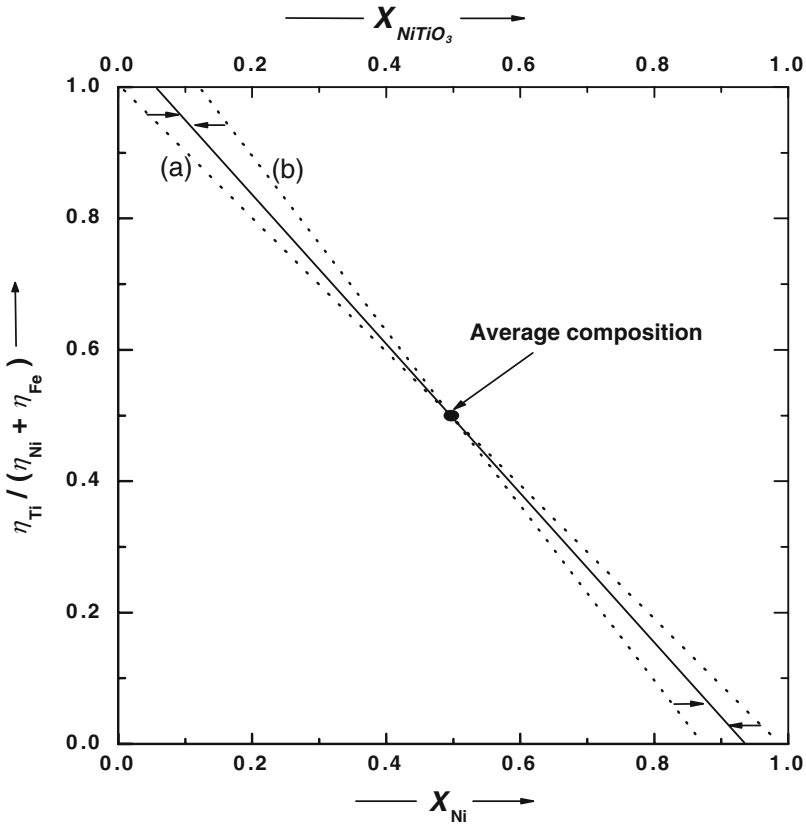

Fig. 4 Illustration of the tie-line rotation technique to check for the attainment of equilibrium

cationic site. The other ions are common and occupy crystallographically distinguishable sites. Activity coefficients of components of the solid solution $FeTiO_3$-$NiTiO_3$ can be derived from the compositions of the oxide-solid solution and the Fe-Ni alloy connected by tie-lines. Each tie-line is defined by the intercrystalline ion-exchange reaction:

$$Fe + NiTiO_3 \rightarrow FeTiO_3 + Ni \qquad \text{(Eq 5)}$$

for which the equilibrium constant K_5 is defined as,

$$K_5 = \frac{a_{Ni} a_{FeTiO_3}}{a_{Fe} a_{NiTiO_3}} = e^{(-\Delta G_5^o/RT)} \qquad \text{(Eq 6)}$$

where ΔG_5^o is standard Gibbs energy change for reaction 5. Expressing each activity as a product of activity coefficient and mole fraction ($a_i = \gamma_i X_i$), and rearranging,

$$K_5 = \left\{ \left(\frac{X_{Ni} X_{FeTiO_3}}{X_{Fe} X_{NiTiO_3}} \right) \left(\frac{\gamma_{Ni}}{\gamma_{Fe}} \right) \left(\frac{\gamma_{FeTiO_3}}{\gamma_{NiTiO_3}} \right) \right\} \qquad \text{(Eq 7)}$$

$$\frac{\gamma_{FeTiO_3}}{\gamma_{NiTiO_3}} = K_5 \left\{ \left(\frac{X_{Fe} X_{NiTiO_3}}{X_{Ni} X_{FeTiO_3}} \right) \left(\frac{\gamma_{Fe}}{\gamma_{Ni}} \right) \right\} \qquad \text{(Eq 8)}$$

The modified Gibbs-Duhem integration technique of Jacob and Jeffes[8] can be used to calculate activity coefficient of a component in the solid solution from the knowledge of the variation of the ratio of activity coefficients with composition across the full composition range. Following the modified technique,

$$\ln \gamma_{FeTiO_3} = \int_1^{X_{FeTiO_3}} X_{NiTiO_3} \, d \ln \left\{ \frac{\gamma_{FeTiO_3}}{\gamma_{NiTiO_3}} \right\} \qquad \text{(Eq 9)}$$

Substituting for the ratio of activity coefficients from Eq 8,

$$\ln \gamma_{FeTiO_3} = \int_1^{X_{FeTiO_3}} X_{NiTiO_3} \, d \ln \left\{ \left(\frac{X_{Fe} X_{NiTiO_3}}{X_{Ni} X_{FeTiO_3}} \right) \left(\frac{\gamma_{Fe}}{\gamma_{Ni}} \right) \right\} \qquad \text{(Eq 10)}$$

Since K_5 is a constant, its actual value does not affect the area under the curve and the evaluation of activity coefficients. The composition ratio on the right side of Eq 10 is calculated from experimentally determined tie-line compositions and the ratio of the corresponding activity coefficients in the alloy phase obtained from the literature.

The Fe-Ni system is well studied and several groups[9-11] have independently assessed the data. The evaluated data sets are in reasonable accord. The data suggested by Chuang et al.[9] appears to be more reliable and has been chosen in this study. At 1273 K, there is a continuous range of solid

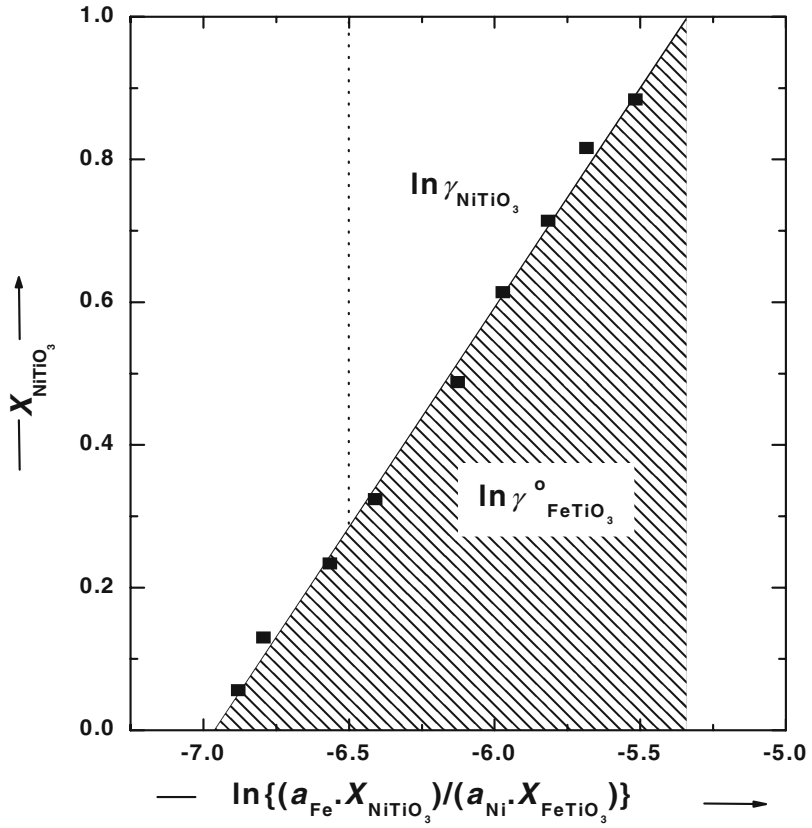

Fig. 5 Integration plot for deriving activity coefficients from tie-line data

Table 2 Activity coefficients of $FeTiO_3$ and $NiTiO_3$ in the oxide solid solution with ilmenite structure at 1273 K obtained by the modified Gibbs-Duhem integration technique

X_{FeTiO_3}	$\ln \gamma_{FeTiO_3}$	$\ln \gamma_{NiTiO_3}$
0.116	0.6342	0.0109
0.184	0.5404	0.0275
0.286	0.4138	0.0664
0.386	0.3060	0.1209
0.512	0.1933	0.2128
0.676	0.0852	0.3709
0.766	0.0444	0.4762
0.870	0.0137	0.6143
0.944	0.0026	0.7233

solution between Fe and Ni with face-centered cubic (fcc) structure. The Gibbs energy of the Fe-Ni solid solution with fcc structure has a small magnetic contribution.[9] Activities exhibit mild negative deviation from Raoult's law.

The modified Gibbs-Duhem integration plot of X_{NiTiO_3} against $\ln\{(X_{NiTiO_3}/X_{FeTiO_3})(a_{Fe}/a_{Ni})\}$ is shown in Fig. 5. A straight line can fit the experimental data within experimental uncertainty. Area under the curve between limits of integration gives the value of $\ln \gamma_{FeTiO_3}$ corresponding to any selected oxide composition. The activity coefficient of $FeTiO_3$ obtained by integration is shown in Table 2 and can be adequately represented by the regular solution model:

$$\ln \gamma_{FeTiO_3} = 0.8116\ (\pm 0.019)\ X^2_{NiTiO_3} \qquad \text{(Eq 11)}$$

Similarly, the activity coefficient of $NiTiO_3$ can be evaluated, as a function of composition, from the area above the curve in Fig. 5:

$$\ln \gamma_{NiTiO_3} = \int_1^{X_{NiTiO_3}} X_{FeTiO_3}\ \mathrm{d} \ln \left\{ \left(\frac{\gamma_{Ni}}{\gamma_{Fe}} \right) \left[\frac{X_{Ni} X_{FeTiO_3}}{X_{Fe} X_{NiTiO_3}} \right] \right\} \qquad \text{(Eq 12)}$$

The activity coefficient of $NiTiO_3$ as a function of composition can be represented as:

$$\ln \gamma_{NiTiO_3} = 0.8116\ (\pm 0.019)\ X^2_{FeTiO_3} \qquad \text{(Eq 13)}$$

The activity-composition relation for ilmenite solid solution at 1273 K is shown in Fig. 6. The components of the oxide solid solution exhibit moderate positive deviations from Raoult's law. The positive deviation is caused by the difference in the ionic radii of the ions Fe^{2+} and Ni^{2+}, which are listed in Table 3.

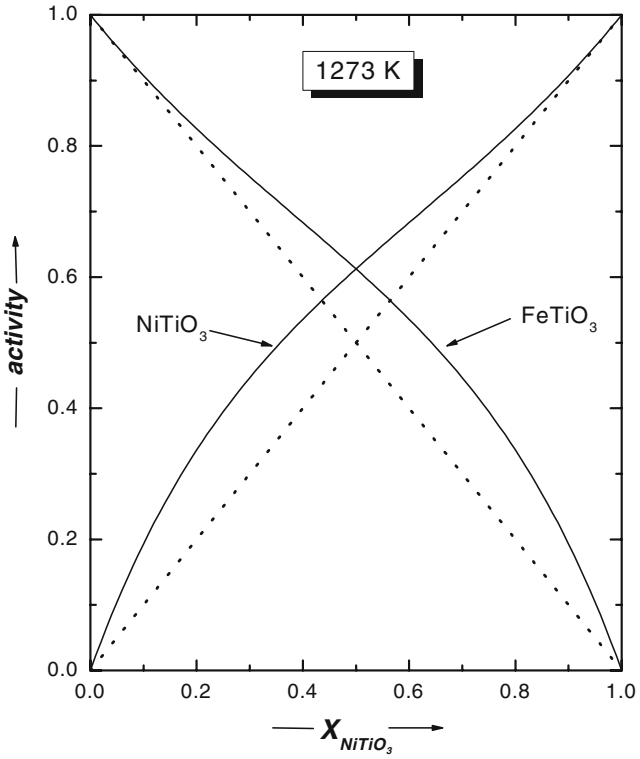

Fig. 6 Variation of activities of $FeTiO_3$ and $NiTiO_3$ in the oxide solid solution with ilmenite structure at 1273 K

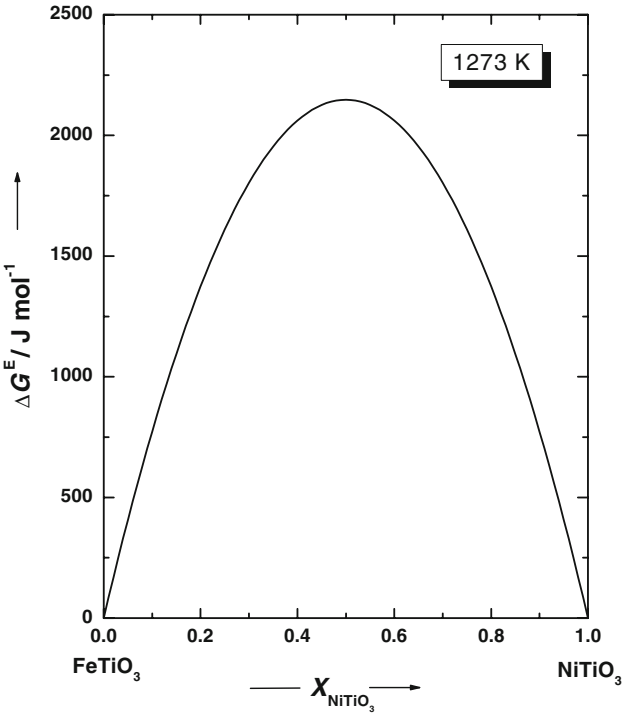

Fig. 7 Variation of excess Gibbs energy of mixing for the $FeTiO_3$-$NiTiO_3$ solid solution at 1273 K

Table 3 Ionic radii of the cations in the ilmenite solid solution

Ion	Ionic radius (CN = 6)	Reference
Ni^{2+}	0.69	[14]
Fe^{2+}	0.74 (a)	[15]
Fe^{3+}	0.645 (a)	[14]
Ti^{3+}	0.67	[14]
Ti^{4+}	0.605	[14]

(a) For high spin (weak field)

The excess Gibbs energy of mixing for the $FeTiO_3$-$NiTiO_3$ solid solution obtained from the two activity coefficients at 1273 K can be represented as:

$$\begin{aligned}\Delta G^{E}_{FeTiO_3-NiTiO_3} &= RT(X_{FeTiO_3}\ln\gamma_{FeTiO_3} + X_{NiTiO_3}\ln\gamma_{NiTiO_3}) \\ &= 0.8116\,(\pm 0.019)\,RT\,X_{FeTiO_3}X_{NiTiO_3} \\ &= 8590\,(\pm 200)\,X_{FeTiO_3}X_{NiTiO_3} \quad \text{J/mol}\end{aligned} \tag{Eq 14}$$

The excess Gibbs energy of mixing is a symmetric function of composition as shown in Fig. 7. Computing values of the equilibrium constant or Gibbs energy change for reaction (5) from each tie-line, one can check the accuracy of the measured compositions. The average value of $K_5 = 474.6$ with an uncertainty (twice the standard deviation) of ±7.1. The value for the Gibbs energy change for the exchange reaction is $\Delta G^{o}_{5} = -65226\ (\pm 160)$ J/mol at 1273 K. The value of standard Gibbs energy is in good agreement with the value of $\Delta G^{o}_{5} = -64353\ (\pm 300)$ J/mol calculated from direct thermodynamic measurements using solid oxide galvanic cells.[6,7]

3.3 Phase Diagram Calculations

Since only Ni-rich compositions ($0 < X_{Fe} < 0.0804$) were involved in experimental studies, it is useful to compute tie-lines for alloys with higher concentration of Fe using the thermodynamic data obtained in this study. The computed tie-lines for the full range of compositions of alloy and oxide solid solution are shown in Fig. 8. The composition variables are mole fractions for alloys and cationic fractions for the oxide solid solution.

The oxygen chemical potential is uniquely defined when Fe-Ni alloys, $FeTiO_3$-$NiTiO_3$ solid solution, and TiO_2 coexist at constant temperature. This oxygen potential ($\Delta\mu_{O_2} = RT\ln p_{O_2}$) is defined by both Eq 1 and 3. Either equation can be used for computation with an appropriate set of activities for the alloy and oxide solid solution. The computed oxygen potentials corresponding to three-phase equilibria at 1273 K are displayed in Fig. 9. It is to be noted that TiO_2 is a nonstoichiometric phase. The maximum oxygen deficiency in TiO_{2-x} at 1273 K is characterized by $x = 0.008$, and this occurs at an oxygen potential of

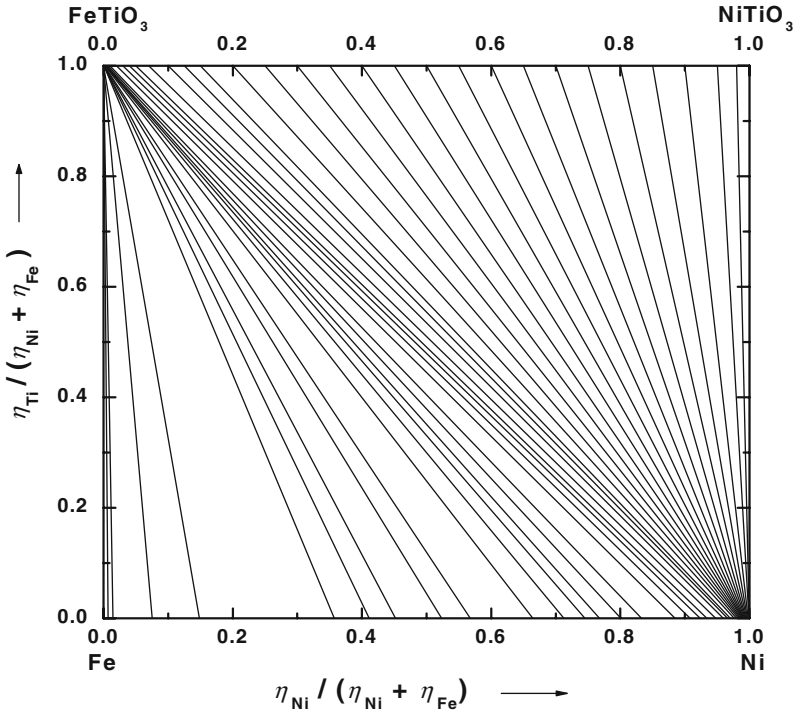

Fig. 8 Full spectrum of computed tie lines between Fe-Ni alloy and $FeTiO_3$-$NiTiO_3$ solid solution at 1273 K

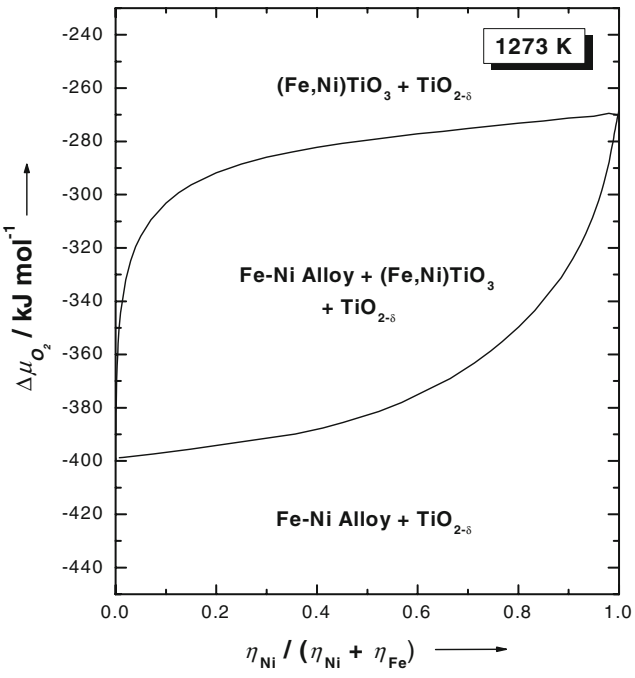

Fig. 9 Variation of oxygen potential for three-phase equilibrium involving the alloy, oxide solution, and TiO_2

$\Delta\mu_{O_2} = -450.93$ kJ/mol.[12] The activity of TiO_2 at this limit of nonstoichiometry assessed from the data of Dirstine and Rosa[13]:

$$\log x = -0.208\ (\pm 0.015)\log p_{O_2} - 5.823\ (\pm 0.225) \quad \text{(Eq 15)}$$

is 0.975. The lowest oxygen potential for three-phase equilibrium in the Fe-Ni-Ti-O quaternary system at 1273 K occurs at $\Delta\mu_{O_2} = -398.82$ kJ/mol corresponding to pure iron. The activity of TiO_2 in the rutile phase corresponding to this oxygen potential is 0.992. Hence, the activity of TiO_2 has been taken as unity in the oxygen potential calculations without introducing a serious error.

3.4 Trace Concentrations of Fe^{3+} and Ti^{3+} in the Ilmenite Phase

The space group of ilmenite $(R\bar{3})$ is a subgroup of the space group $(R\bar{3}\,2/c)$ of corundum and hence solid solutions can form between the titanate phases with ilmenite structure and αFe_2O_3 and Ti_2O_3, which have the corundum structure, if ionic sizes are favorable. Both structures are characterized by hexagonal close packing of oxygen ions with cations occupying two-thirds of the octahedral positions. In the ilmenite structure, the cations order in alternate layers perpendicular to the c axis. Thus, the structure of ilmenite is a superstructure of the basic corundum type. The ionic radii of the different ions for sixfold coordination from Shannon[14] are listed in Table 3. In a solid solution involving corundum and ilmenite phases, order can appear gradually as a higher-order phase transition.

The activity of Fe_2O_3 in the ilmenite solid solution corresponding to three-phase equilibrium can be calculated using:

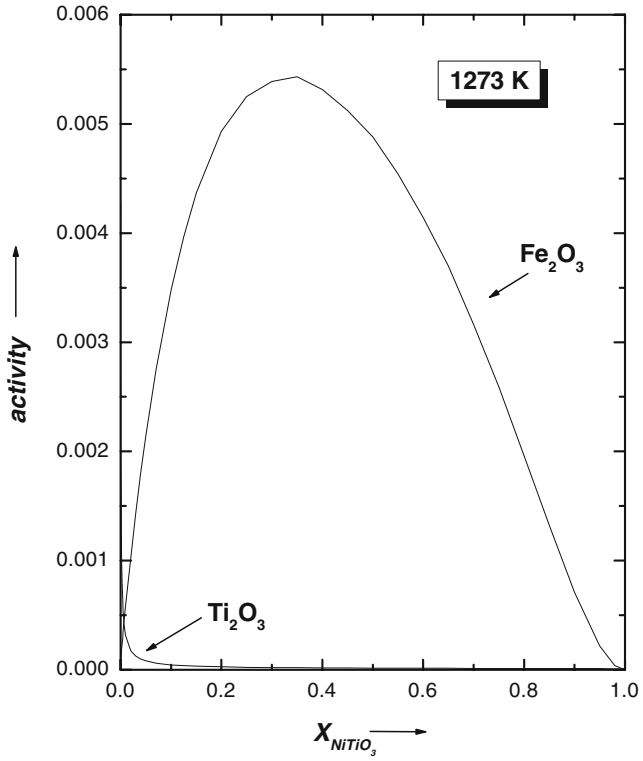

Fig. 10 Variation of activity of M_2O_3 (M = Fe, Ti) with composition of titanate solid solution at oxygen potential defined by three-phase equilibrium at 1273 K

$$2Fe + {}^{3}/_{2}O_2 \rightarrow Fe_2O_3 \qquad \text{(Eq 16)}$$

Standard Gibbs energy change for the reaction at 1273 K taken from Ref 16 can be expressed as:

$$\Delta G^{o}_{16} = -RT \ln\left(\frac{a_{Fe_2O_3}}{a^2_{Fe}.p^{3/2}_{O_2}}\right) = -493,510 \text{ J/mol} \qquad \text{(Eq 17)}$$

The activity of Fe is obtained from alloy composition and thermodynamic data for the binary Fe-Ni system.[9] The oxygen potential for three-phase equilibrium at 1273 K has already been evaluated (Fig. 9). The variation of the activity of Fe_2O_3 with composition of the titanate solid solution at oxygen potentials defined by three-phase equilibria is displayed in Fig. 10.

The activity of Ti_2O_3 in the titanate solid solution is defined by the reaction,

$$2Ti_2O_3 + O_2 \rightarrow 4TiO_2 \qquad \text{(Eq 18)}$$

The standard Gibbs energy change for the reaction at 1273 K from NIST-JANAF Thermochemical tables[17] can be expressed as:

$$\Delta G^{o}_{18} = -RT \ln\left(\frac{a^4_{TiO_2}}{a^2_{Ti_2O_3} \times p_{O_2}}\right) = -514,590 \text{ J/mol} \qquad \text{(Eq 19)}$$

Table 4 Estimated regular solution parameters, activity coefficients at infinite dilution of M_2O_3 (M = Fe, Ti) in the pure ilmenite phases, and the estimated concentration of M_2O_3 in $NiTiO_3$ and $FeTiO_3$ at oxygen potentials for three-phase equilibrium at 1273 K

Solid solution	Interaction parameter (Ω), J/mol	Activity coefficient, $\gamma^{o}_{M_2O_3}$	Concentration, $X_{M_2O_3}$
$NiTiO_3$-Fe_2O_3	16,280	4.7	0
$NiTiO_3$-Ti_2O_3	16,285	4.7	0.0014
$FeTiO_3$-Fe_2O_3	24,950	10.6	0.0020
$FeTiO_3$-Ti_2O_3	24,950	10.6	0.0198

The variation of the activity of Ti_2O_3 with composition of the titanate solid solution is displayed in Fig. 10. The activity is evaluated at partial pressures of oxygen defined by the three-phase equilibrium at 1273 K.

The concentration of Fe^{3+} and Ti^{3+} ions in the ilmenite solid solution can be estimated from the activities of Fe_2O_3 and Ti_2O_3. The activity coefficients of Fe_2O_3 and Ti_2O_3 at infinite dilution in the ilmenite phases can be estimated using the regular solution model for mixing on each cation site. The value of the regular solution parameters listed in Table 4 for different solid solutions were estimated based on differences in ionic radii.

For a solution of 1 in 2,

$$\Delta\overline{G}^{E}_1 = \Omega X^2_2 = RT \ln\gamma_1 \qquad \text{(Eq 20)}$$

For a dilute solution of 1 in 2 ($X_2 \approx 1$), Eq 20 can be re-written as,

$$\Omega = RT \ln\gamma^{o}_1 \qquad \text{(Eq 21)}$$

The concentrations of Fe^{3+} and Ti^{3+} ions in pure $FeTiO_3$ and $NiTiO_3$, estimated from the activities of Fe_2O_3 and Ti_2O_3 are summarized in Table 4. Since these concentrations are small, the derived activities of $FeTiO_3$ and $NiTiO_3$ in the titanate solid solution are probably not affected significantly.

4. Conclusions

Although thermodynamic properties of Fe-Ni alloys exhibit mild negative deviations from Raoult's law, activities in the $FeTiO_3$-$NiTiO_3$ solid solution exhibit moderate positive deviations from ideality. Formation of the oxide solid solution involves the mixing of Fe^{2+} and Ni^{2+} ions. The dissimilar behavior of alloy and oxide solid solution is indicative of the difference in the nature of bonding in the two phases. Thermodynamic properties of the alloy are determined primarily by the variation of Fermi energy with composition and possible charge transfer between the Wigner-Sietz cells of Fe and Ni. Thermodynamic properties of the oxide solid solution are more influenced by the ionic size mismatch between the next-nearest neighbor divalent

cations and resulting distortion of the lattice. The nearest-neighbor environment around the divalent cations remains virtually the same, unlike in the case of alloys.

References

1. P.K. de Bokx, R.L.C. Bonne, and J.W. Geus, Strong Metal-Support Interaction in Ni/TiO_2 Catalysts: The Origin of TiO_x Moieties on the Surface of Nickel Particles, *Appl. Catal.*, 1987, **30**(1), p 33-46
2. P.H.M. de Korte and G. Blasse, Water Photoelectrolysis Using Nickel Titanate and Niobate as Photoanodes, *J. Solid State Chem.*, 1982, **44**, p 150-155
3. D.S. Ginley and M.A. Butler, The Photoelectrolysis of Water Using Iron Titanate Anodes, *J. Appl. Phys.*, 1977, **48**(5), p 2019-2021
4. D.J. Taylor, P.F. Fleig, and R.A. Page, Characterization of Nickel Titanate Synthesized by Sol-Gel Processing, *Thin Solid Films*, 2002, **408**, p 104-110
5. L.G. Evans and A. Muan, Activity-Composition Relations of Solid Solution of Manganese and Nickel Titanates at 1250 °C as Derived from Equilibria in the Systems MnO-CoO-TiO_2 and MnO-CoO-TiO_2, *Thermochim. Acta*, 1971, **2**(4), p 277-298
6. G.M. Kale and K.T. Jacob, Chemical Potential of Oxygen for Iron-Rutile-Ilmenite and Iron-Ilmenite-Ulvospinel Equilibria, *Metall. Trans. B*, 1992, **23B**, p 57-64
7. K.T. Jacob, V.S. Saji, and S.N.S. Reddy, Thermodynamic Evidence for Order-Disorder Transition in $NiTiO_3$, *J. Chem. Thermodyn.*, 2007, **39**, p 230-235
8. K.T. Jacob and J.H.E. Jeffes, An improved Method for Calculating Activities from Distribution Equilibria, *High Temp.—High Press.*, 1972, **4**, p 177-182
9. Y.-Y. Chuang, Y.A. Chang, and R. Schmid, A Thermodynamic Analysis of the Phase Equilibria of the Fe-Ni System above 1200 K, *Metall. Trans. A*, 1986, **17A**, p 1373-1380
10. A. Gabriel, P. Gustaffson, and I. Ansara, A Thermodynamic Evaluation of the C-Fe-Ni System, *Calphad*, 1987, **11**, p 203-218
11. B.-J. Lee, Revision on Thermodynamic Descriptions of the Fe-Cr and Fe-Ni Liquid Phases, *Calphad*, 1993, **17**(3), p 251-268
12. K.T. Jacob, S.M. Hoque, and Y. Waseda, Synergistic Use of Thermogravimetric and Electrochemical Techniques for Thermodynamic Study of TiO_x ($1.67 \leq x \leq 2.0$) at 1573 K, *Mater. Trans. JIM*, 2000, **41**(6), p 681-689
13. R.T. Dirstine and C.J. Rosa, Defect Structure and Related Thermodynamic Properties of Nonstoichiometric Rutile (TiO_{2-x}) and Nb_2O_5 Doped Rutile. Part I: The Defect Structure of TiO_{2-x} (Rutile) and Partial Molar Properties for Oxygen Solution at 1273 K, *Z. Metallkd.*, 1979, **70**(6), p 372-378
14. R.D. Shannon, Revised Effective Ionic Radii and Systematic Studies of Interatomic Distances in Halides and Chalcogenides, *Acta Crystallogr.*, 1976, **A32**, p 751-767
15. H.St.C. O'Neill and A. Navrotsky, Simple Spinels: Crystallographic Parameters, Cation Radii, Lattice Energies, and Cation Distribution, *Am. Mineral.*, 1983, **68**, p 181-194
16. B. Sundman, An Assessment of the Fe-O System, *J. Phase Equilibria*, 1991, **12**(1), p 127-140
17. M.W. Chase, Jr., NIST-JANAF Thermochemical Tables, *J. Phys. Chem. Ref. Data,* 1998, Monograph No. 9